Agricultural and Forest Meteorology 200 (2015) 46–56

Contents lists available at ScienceDirect

Agricultural and Forest Meteorology

journal homepage: www.elsevier.com/locate/agrformet

Modeling the seasonal dynamics of leaf area index based on environmental constraints to canopy development

Philip Savoy*, D. Scott Mackay

Department of Geography, State University of New York at Buffalo, Buffalo, NY 14261, United States

ARTICLE INFO

Article history:
Received 22 April 2014
Received in revised form
18 September 2014
Accepted 21 September 2014

Keywords:
Leaf area index (LAI)
Modeling
Phenology

ABSTRACT

Leaf area index (LAI) is an important variable for understanding land-surface atmosphere flux dynamics and a key biophysical variable included in terrestrial biosphere models. Because of its influence on resource cycling and atmospheric feedbacks it is necessary to have a model that can accurately predict the seasonal progression of canopy development. The goal of this study is to use a simple function to modify a prognostic phenology model, based on the influence of environmental factors on limiting foliar phenology, into a model capable of predicting the seasonal course of LAI. Model performance was assessed by comparison to a time-series of LAI measurements derived from gap fraction theory at five deciduous sites selected from the FLUXNET database. The model was assessed in terms of its ability to predict the magnitude of LAI as well as phenological transition dates. The results show a strong correlation between predicted LAI and gap fraction derived estimates ($r = 0.94$, RMSE = 0.45). The accuracy of the model varied among sites at predicting transition dates but remained consistently high at predicting the continuous seasonal progression of LAI. Our results demonstrate that a simple prognostic phenology model can be rescaled to predict the seasonal course of LAI in deciduous forests.

1. Introduction

A link between climate change and phenology, i.e. the study of the timing of seasonal cycles in relation to biotic and abiotic forces (Lieth, 1974), has been documented across a wide range of taxa and geographical locations (Menzel et al., 2006; Parmesan, 2006; Schwartz et al., 2006); the resulting changes in the phenology of forests have important implications for ecosystem productivity (Dragoni et al., 2011; Myneni et al., 1997; Richardson et al., 2010). In addition to phenology, the associated seasonal patterns of canopy development are also an important component of CO_2 fluxes (Randerson et al., 1997). Leaf area index (LAI), defined as half the total leaf surface area per unit ground surface (Chen and Black, 1992), is a useful measure of seasonal canopy dynamics. The seasonal progression of LAI influences canopy conductance (Blanken and Black, 2004; Sakai et al., 1997), albedo (Sakai et al., 1997), sensible and latent heat fluxes (Moore et al., 1996), CO_2 fluxes (Randerson et al., 1997), and surface air temperatures (Fitzjarrald et al., 2001; Levis and Bonan, 2004). LAI is thus a key variable in computing land-surface atmosphere flux dynamics, and an important biophysical variable included in a number of terrestrial biosphere models. Since canopy seasonality is an important component of carbon (C) fluxes, poor representation of the seasonal dynamics of LAI can lead to errors in vegetation productivity (Kucharik et al., 2006; Ryu et al., 2008). In order to understand and model impacts of climatic conditions on ecosystems it is essential to not only have accurate representation of vegetation phenology, but also the associated seasonal dynamics of LAI. Despite the importance of LAI in terrestrial biosphere models, its representation in these models has been insufficient (Richardson et al., 2012).

There are generally three approaches for modeling the seasonality of LAI in terrestrial biosphere models: prescribed, prognostic, and hybrid models that combine these two approaches (Richardson et al., 2012). Prognostic LAI models are preferable because they allow for forecasting under future climate scenarios. Prognostic models have the potential to behave more realistically than prescribed methods because leaf emergence occurs during periods of favorable environmental conditions for photosynthesis (Levis and Bonan, 2004). Several examples of prognostic LAI models are based on the relationship between vegetation and environmental conditions. Growing degree days (GDD) have been used to predict phenological events such as budburst (Hunter and Lechowicz, 1992; Jeong et al., 2012) and to model LAI (Levis and Bonan, 2004). The growing season index (GSI) (Jolly et al., 2005) is a more flexible generalized indicator of phenology than GDD because it computes the limitations imposed on plant phenology by temperature, soil

* Corresponding author. Tel.: +1 716 645 0471.
E-mail address: psavoy@buffalo.edu (P. Savoy).

http://dx.doi.org/10.1016/j.agrformet.2014.09.019
0168-1923/

Table 1
Site locations, characteristics, and years of data availability.

Descriptor	Site name (site ID)				
	SSA Old aspen (Ca-Oas)	Harvard forest (US-Ha1)	Morgan Monroe state forest (US-MMS)	Univ. of Mich. Biological Station (US-UMB)	Willow Creek (US-WCr)
Location					
Lat	53.63	42.54	39.32	45.56	45.81
Lon	−106.20	−72.17	−86.41	−84.71	−90.08
Elevation (m)	601	340	275	243	520
Site description					
Climate	Boreal	Temperate	Temperate	Temperate	Temperate
IGBP	DBF	DBF	DBF	DBF	DBF
Canopy height (m)	21.5	23	25–27	22	24
Stand age (yrs)*	87	84	75–85	85	65–90
Sand, silt, clay (%)	20, 65, 15	66, 29, 5	34, 3, 63	92, 7, 1	54, 33, 13
Dominant vegetation (overstory)	Trembling Aspen, Balsam Poplar	Red Oak, Red Maple, Black Birch, White Pine, Eastern Hemlock	Sugar Maple, Tulip Poplar, Sassafras, White Oak, Black oak	Bigtooth Aspen, Trembling Aspen	Sugar Maple, Basswood, Green Ash
Study period mean annual meteorological values					
Air temperature (°C)	2.2	7.9	12.7	7.6	6.1
VPD (kPa)	0.36	3.3	5.03	4.1	2.05
Precipitation (mm)	461	1138	1108	589	749
Years of data available					
Meteorological	1997–2006	1992–2006	2001–2003; 2005–2006	1999–2006	1999–2006
PAR	1997–2006	1992–2006	2001–2006	2002–2007	1999–2006
LAI-2000	1998–2006	1998–'99; 2005–'06	2001–2006	1999–2006	NA
References	Barr et al. (2004, 2007), Black et al. (2000)	Urbanski et al. (2007)	Dragoni et al. (2011), Schmid et al. (2000)	Gough et al. (2013)	Cook et al. (2004)

* Approximate mean stand age in 2006.

water via its complementarity with atmospheric vapor pressure deficit (VPD), and photoperiod. Since GSI models the effects of environmental constraints on canopy development, it has proven to be useful as a prognostic model of LAI. Consequently, there is a growing body of literature using GSI as a basis for predicting LAI (Groenendijk et al., 2011; Stöckli et al., 2008; Zhang et al., 2012).

Typically phenology is studied by examining the timing of discrete events. In deciduous broad leaf forests the seasonal progression of canopy dynamics is demarcated by phenological events such as budburst, leaf development, senescence, and abscission. However, in order to thoroughly test the ability of the GSI framework to predict the seasonality of LAI it is necessary to test it against continuous observations. Remote sensing platforms can monitor both phenology and the seasonality of canopy dynamics. Remote sensing of phenology, often referred to as land surface phenology (LSP), can monitor changes in vegetation phenology through the derivation of a number of metrics (Moulin et al., 1997; Reed et al., 1994; White et al., 2009; White et al., 1997). Despite the recent improvements with the Moderate Resolution Imaging Spectroradiometer (MODIS) C5 LAI product (De Kauwe et al., 2011; Fang et al., 2012), there are still uncertainties in point-to-pixel comparisons of LAI, primarily due to landcover heterogeneity within mixed pixels (Chen et al., 2002). Because of the spatial and temporal scale discrepancies between ground and remote sensing measurements, it is preferable to use input and validation data that are of similar scales.

The FLUXNET database (www.fluxdata.org) provides a unique opportunity to test LAI predictions made using the GSI framework because it provides both tower-based input meteorological variables, necessary to calculate GSI, and photosynthetically active radiation (PAR) sensors capable of generating high frequency measurements of LAI (Richardson et al., 2012). We used this dataset to derive the complete seasonal progressions of canopy dynamics, as well as to extract metrics that quantified seasonal patterns in phenology. By testing the GSI framework against high frequency in situ measurements of LAI we can determine its limitations and assess its potential for improving seasonal LAI dynamics in ecosystem models.

In this paper we seek to test a simple model for leveraging the GSI framework into a prognostic model of LAI. To assess the performance of GSI at deciduous broadleaf sites, we test several formulations of GSI by varying the combinations its three environmental components. Specifically the objectives are: (1) test the ability of a simple single parameter function to rescale GSI into predicted LAI; (2) test the ability of a single study-wide parameter estimate and best GSI model formulation to predict LAI; and (3) compare the performance of site-specific parameter estimation and selection of model formulation to the study-wide model. To accomplish these objectives we tested model performance against periodic in situ LAI measurements, high frequency LAI estimated from PAR data, and phenological transition dates derived from these estimates.

2. Data and methods

2.1. Study sites and data

Five test sites were selected from the FLUXNET network based on the presence of validation data as well as their inclusion in complementary studies (Melaas et al., 2013; Richardson et al., 2012). The selected sites were all deciduous broad leaf forests of similar stand ages, but varied in species composition and environmental conditions (Table 1). GSI requires three environmental inputs for its calculation; temperature, VPD, and photoperiod. Tower-based gap-filled air temperature and VPD data were obtained through the

AmeriFlux (http://public.ornl.gov/ameriflux/dataproducts.shtml) and Fluxnet-Canada (http://fluxnet.ornl.gov/site_list/Country/CA) data networks for each of the sites resulting in 46 site years of meteorological data. Photoperiod was calculated based on latitude and the time of year (Campbell and Norman, 1998).

Predicted LAI values were compared to periodic in situ measurements of LAI and daily LAI derived from tower-based above and below canopy photosynthetically active radiation (PAR) sensors. A full complement of validation data was not available for all of the sites and thus analysis at each of the sites was restricted accordingly (Table 1). In situ LAI-2000 plant canopy analyzer (Li-Cor Biosciences, Lincoln, NE, USA) measurements published in the respective databases were used to test the accuracy of the model at predicting the magnitude of LAI. When appropriate, LAI-2000 measurements were adjusted from plant area index (PAI) to LAI by subtracting the minimum leaf off measurement from all measurements. Because the frequency of LAI-2000 measurements varied between sites, and there was not always a leaf off measurement present for each year, a single minimum leaf off value was chosen from the total pool of measurements available at each respective site. LAI-2000 measurements were not present for all sites or years nor were they made frequently enough to serve as validation for phenological transition dates or intra-annual patterns of LAI.

Gap fraction theory was used to derive daily values of LAI from the ratio of below canopy to above canopy photosynthetically active radiation (PAR) (Richardson et al., 2012; Wythers et al., 2003) and served as reference for both the magnitude of LAI and the timing of phenological transition dates. Daily LAI estimates tended to exhibit noise, represented by erroneously high values, during periods of dormancy. During periods of dormancy the lower 20% quantile of LAI values was calculated, and only points within 0.5 of this value were retained. Filtering was applied only to periods of dormancy, and no points were removed at other portions of the year. A spline was fit through each year of data in order to extract the seasonal pattern of canopy progression (Fig. 1a). The spline was then rescaled so that the minimum value was zero and the seasonal maximum was equal to 90% of the highest observed LAI-2000 measurement for each study site. At US-WCr the site LAI value reported by AmeriFlux was used to represent LAI_{MAX} since no LAI-2000 measurements were available. Rescaling using 90%, instead of 100% of the maximum observed LAI, was chosen because it produced a smaller root mean squared error (RMSE) when compared to LAI-2000 measurements and reduced overestimation of LAI. Fig. 1b shows an example of the rescaled PAR derived LAI values (LAI_{PAR}) at US-MMS. Only four of the sites had both LAI-2000 measurements and below canopy PAR data available, but the relatively strong correlations at, Ca-Oas ($r = 0.93$), US-Ha1 ($r = 0.88$), US-MMS ($r = 0.96$) and US-UMB ($r = 0.93$) suggest that the methodology as implemented can be extended to US-WCr and used as an additional source of validation data at these five sites.

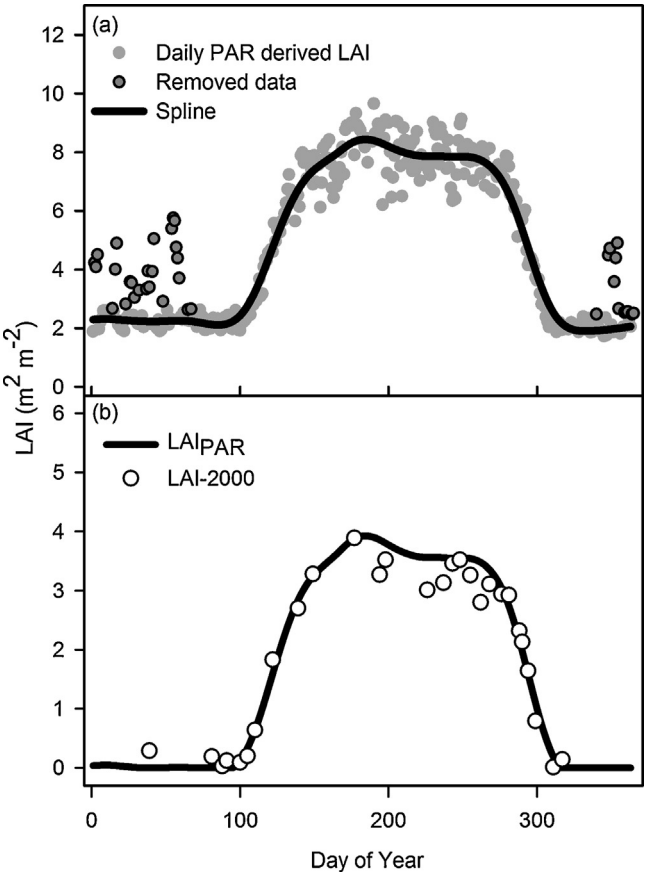

Fig. 1. (a) An example of processing the daily leaf area index (LAI) derived from above and below canopy photosynthetically active radiation (PAR) for 2003 at US-MMS. Noisy data during periods of canopy senescence were removed and then a spline was fit through the data in order to extract the overall pattern of canopy development. (b) The final rescaled LAI values derived from gap fraction theory (LAI_{PAR}) plotted with observed LAI-2000 measurements.

2.2. The growing season index (GSI)

In the GSI model each environmental variable is transformed into an index value, ranging from 0 to 1, that denotes its inhibition to canopy development. Threshold values were used to determine where an environmental variable was completely limiting to development (index value of 0) and where it was no longer limiting to development (index value of 1). We used the lower ($T_{min} = -5\,^{\circ}C$) and upper ($T_{max} = 10\,^{\circ}C$) temperature threshold values suggested by Thompson et al. (2011) instead of the $-2\,^{\circ}C$ and $5\,^{\circ}C$ presented in Jolly et al. (2005) because testing revealed better performance of the former. Each environmental variable used in the formulation of GSI was transformed according to the following set of equations:

$$f_1(T_a) = \begin{cases} 0, & T_a \le T_{min} \\ \dfrac{T_a - T_{min}}{T_{max} - T_{min}}, & T_{max} > T_a > T_{min} \\ 1, & T_a \ge T_{max} \end{cases} \quad (1)$$

$$f_2(Photo) = \begin{cases} 0, & Photo \le Photo_{min} \\ \dfrac{Photo - Photo_{min}}{Photo_{max} - Photo_{min}}, & Photo_{max} > Photo > Photo \\ 1, & Photo \ge Photo_{max} \end{cases} \quad (2)$$

$$f_3(VPD) = \begin{cases} 0, & VPD \ge VPD_{max} \\ 1 - \dfrac{VPD - VPD_{min}}{VPD_{max} - VPD_{min}} & VPD_{max} > VPD > VPD_{min} \\ 1, & VPD \le VPD_{min} \end{cases} \quad (3)$$

where T_a is the minimum daily air temperature, *Photo* is the daily photoperiod, and *VPD* is the mean daily vapor pressure deficit VPD. Threshold values are represented by T_{min}, T_{max}, $Photo_{min}$, $Photo_{max}$, VPD_{min}, and VPD_{max} (Jolly et al., 2005). The daily product of the three index values was taken, resulting in a daily indicator value (*DGSI*),

Table 2
Different model formulations of the growing season index (GSI) framework. The combination of functions that each model is comprised of are denoted by its subscript letters: where T is air temperature ($f_1(T_a)$), P is photoperiod ($f_2(Photo)$), and D is vapor pressure deficit ($f_3(VPD)$).

Model	$f_1(T_a)$	$f_2(Photo)$	$f_3(VPD)$	Parameters
$L_{(T)}$	X			2
$L_{(T,P)}$	X	X		4
$L_{(T,D)}$	X		X	4
$L_{(T,P,D)}$	X	X	X	6

and then a moving 21 day mean was used to compute the GSI so as to account for day-to-day variations in environmental conditions:

$$DGSI = f_1(T_a) \times f_2(Photo) \times f_3(VPD) \quad (4)$$

$$GSI_i = \frac{\left(DGSI_i + DGSI_{i-1} + DGSI_{i-2} + \cdots + DGSI_{i-(21-1)}\right)}{21} \quad (5)$$

Because the sites included in the study were all primarily temperature driven, we also tested a number of formulations of the GSI model. The different formulations of the model were calculated by varying the functions used to calculate *DGSI* (Table 2). This was done in order to determine if the inclusion of additional functions showed improvement beyond a simple model driven solely by temperature. Each of the four model formulations was applied to the pooled study-wide dataset, as well as individually at each site. By applying the models to study-wide data, as well as at individual sites, we were able to compare between the best study-wide formulation and the best site-specific formulations.

2.3. Predicting LAI from GSI

Groenendijk et al. (2011) used a linear rescaling approach to calculate LAI from GSI by taking the product of GSI and the maximum observed LAI value. However, Jolly et al. (2005) indicated that they determined leaf onset occurred when GSI reached a value of 0.5. Consequently, when GSI is less than 0.5 it can be inferred that LAI would be 0 in deciduous forests. Jolly et al. (2005) chose 0.5 for the threshold value to initiate budburst, but suggested that it may vary based on vegetation type and encouraged further testing. Instead of performing a linear rescaling of GSI to predict LAI we performed rescaling using a piecewise linear function based on a threshold:

$$L = \begin{cases} 0, & GSI < \tau \\ GSI \times 0.9LAI_{\max}, & GSI \geq \tau \end{cases} \quad (6)$$

where LAI_{max} is the maximum observed LAI at a site, τ is the value of GSI required to initiate leaf onset in the spring and offset in the fall, and L is the predicted LAI based on rescaling the GSI phenology model. The value of τ impacts the way in which GSI is rescaled to LAI by influencing both the timing of leaf onset and offset, and also the rate of green up and senescence. Increasing the threshold value will delay leaf onset and increase the rate at which LAI increases (Fig. 2).

2.4. Parameter estimation, model selection, testing and validation

The estimation of τ was based on minimizing the residual sum of squares (RSS) between predicted LAI and LAI_{PAR}. Estimation of τ was done across all sites and years of data to generate a single study-wide best estimate. In addition, τ was estimated individually at each site to compare the performance of site-specific versus study-wide estimation.

Because the sites included in the study are all primarily temperature driven, we tested a number of formulations of the GSI model framework to determine if there was improvement over a simple model of temperature. The Akaike information criterion corrected for small datasets (AICc) was used to identify the best model formulation because it encompasses trade-offs between model parsimony and fit (Burnham, 2002). AICc incorporates an additional bias correction term over AIC. It is often recommended AICc be used for practical purposes because as the sample size (n) increases compared to the number of parameters (K) it will converge to be equivalent to AIC (Burnham, 2002).

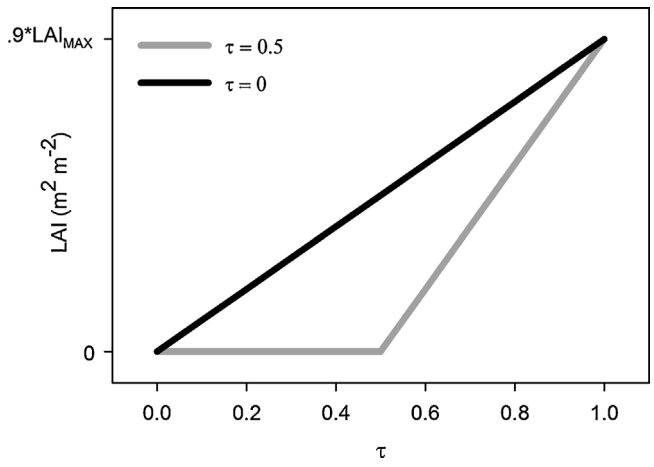

Fig. 2. An illustration of how varying the cutoff value (τ), in the piecewise linear function used to rescale the growing season index (GSI) to leaf area index (LAI), influences the rate at which GSI is rescaled to LAI.

Pearson's correlation coefficient (r) was used to assess the correlation between predicted and observed values of LAI derived from both in situ LAI-2000 measurements and LAI_{PAR}. Because r can be high even when the magnitudes differ, the ability of L to accurately predict the magnitude of LAI was measured by calculating the root mean squared error (RMSE) between predicted and observed LAI values. RMSE provides a measure of the magnitude of errors between observed and predicted LAI. Due to the differing sample size and frequency between the two sets of validation data, comparisons to LAI-2000 data were done on a site by site basis whereas comparisons to LAI_{PAR} were done on a yearly basis in each site.

In addition to testing the ability to predict the magnitude of leaf area, we also tested the capability to predict phenological transition dates. Relative thresholds of 20%, 50%, and 80% of the seasonal peak in LAI were chosen to represent several points along the seasonal progression of canopy development and to provide a point of comparison to previous studies (Richardson et al., 2012). Transition dates were extracted, for both predicted and observed data, by finding the first date in the spring and last date in the fall where LAI crossed each threshold. Bias in the model predictions were calculated by subtracting the observed date from the predicted date and the mean bias for each transition threshold was then calculated for each site as well as across all sites and years. The mean bias was also calculated across the 20%, 50%, and 80% for the spring and for the fall to summarize the overall bias in each of the two seasons.

3. Results

3.1. Piecewise versus linear rescaling of leaf area index

In order to provide comparison to the original GSI framework, the $L_{(T,P,D)}$ model was selected to estimate the value of τ based on study-wide comparisons between predicted LAI and LAI_{PAR}. A range of values for τ were chosen in order to demonstrate the

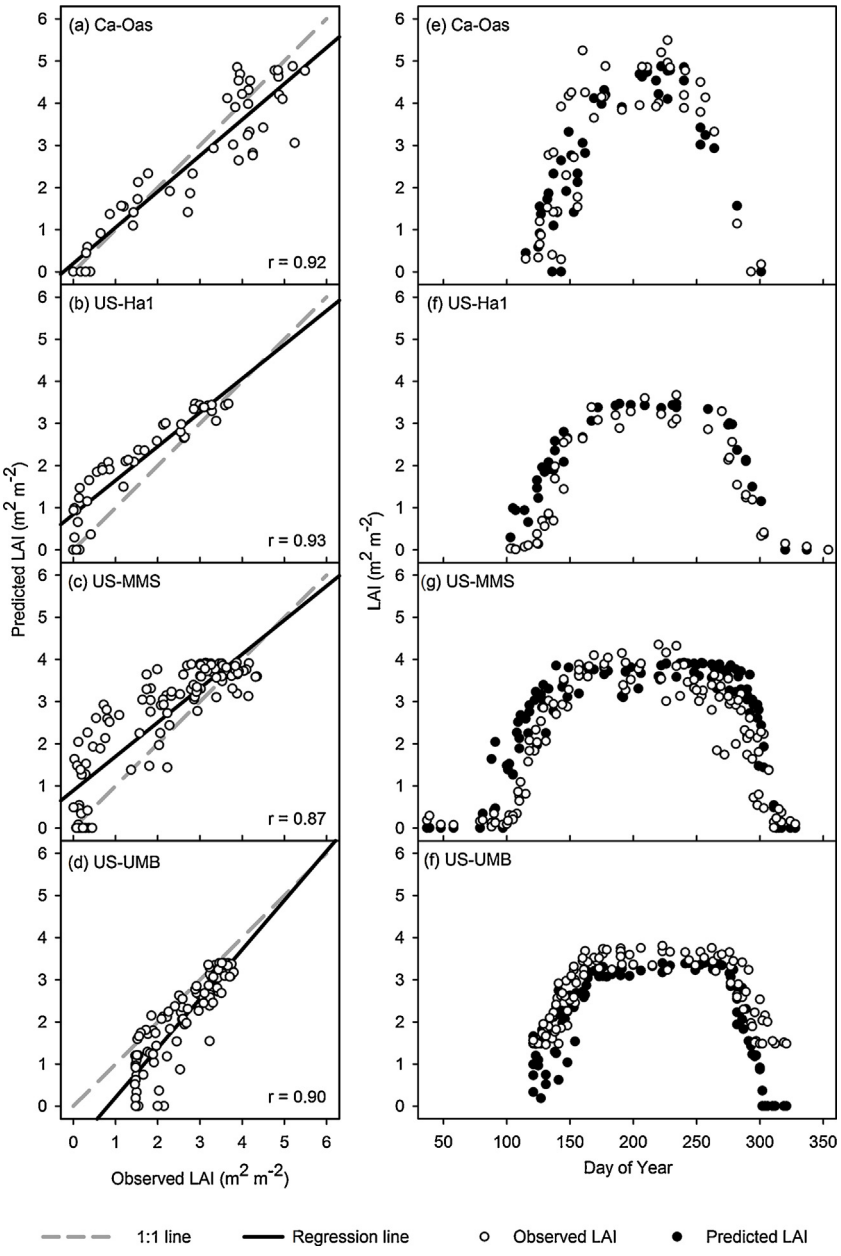

Fig. 3. The relationship between observed and predicted leaf area index (LAI) values for (a) Ca-Oas, (b) US-Ha1, (c) US-MMS, and (d) US-UMB. Plots (e)–(f) show a temporal view of the data presented in (a)–(d). Field observations using the LAI-2000 plant canopy analyzer were obtained from the respective databases to serve as observations. Predicted LAI was generated by rescaling the growing season index (GSI) phenology model to LAI. Values of predicted LAI are for the study-wide estimated parameter τ and model formulation ($L_{(T,P,D)}$; $\tau = 0.39$).

influence of τ on study wide fitting statistics (Table 3). At $\tau = 0.4$ all sites, except US-UMB, showed reduced RMSE and increased r when compared to LAI-2000 measurements. Linear rescaling ($\tau = 0$) and piecewise rescaling of $L_{(T,P,D)}$ were both comparable in their performance for average study-wide comparisons to LAI_{PAR}, however, there was variation in their performance at individual sites. At US-WCr mean RMSE was reduced from 1.07 at $\tau = 0$ to 0.59 at $\tau = 0.4$. Piecewise rescaling also showed a 1 week reduction in the mean absolute error (MAE) in study wide phenological transition dates. US-Ha1, US-MMS, US-UMB, and US-WCr all showed 12 day reductions in MAE of phenological transition dates when compared to linear rescaling. Mean bias across spring transition thresholds was reduced from −29 (±16 days) to −10 (±14 days) by using piecewise linear rescaling of LAI, with the 20% threshold having a 28 day reduction in bias.

3.2. Study-wide τ estimation and best model formulation

Across all sites and years τ was estimated for each of the model formulations used to predict LAI. Each of the model formulations estimated the same value of τ, thus the best τ was independent of model formulation. The model with the lowest AICc value was $L_{(T,P,D)}$ with $\tau = 0.39$. This model formulation and τ will be referred to as the study-wide model in the following sections.

3.2.1. Comparison to in situ LAI-2000 measurements

Predicted LAI was compared directly to LAI-2000 measurements of the same day and year for each of the four sites where in situ measurements were present. US-Ha1 displayed the strongest correlation and lowest error ($r = 0.93$, RMSE = 0.71) compared to LAI-2000 measurements among the four sites (Fig. 3), however, the

Table 3
Study wide fitting statistics for different values of the parameter (τ) used in piecewise linear rescaling of the growing season index (GSI) to leaf area index (LAI). All results are presented for the full formulation of the model ($L_{(T,P,D)}$) (Table 2). LAI_{PAR} is the continuous LAI dataset estimated from photosynthetically active radiation (PAR) sensors.

τ	Relation to LAI_{PAR}		Transition dates	
	r	RMSE	Bias	MAE
0	0.91	0.79	−13	20
0.1	0.92	0.72	−12	18
0.2	0.93	0.65	−10	15
0.3	0.94	0.61	−9	14
0.4	0.94	0.59	−8	13
0.5	0.94	0.62	−7	12
0.6	0.92	0.71	−5	13
0.7	0.90	0.86	−4	16
0.8	0.84	1.07	−3	21
0.9	0.74	1.41	0	29

model performed consistently across all sites. At US-UMB LAI was underestimated during periods of low LAI, such as at the start and the end of the growing season, but performed better at predicting values in the middle of the growing season.

3.2.2. Comparison to LAI_{PAR}

The patterns of canopy dynamics predicted by $L_{(T,P,D)}$ were in good agreement with LAI_{PAR} for all sites and years ($r \geq 0.83$). Across all site-years of data $L_{(T,P,D)}$ displayed a strong mean correlation ($r = 0.95$, RMSE = 0.55) to LAI_{PAR}. All sites had mean correlations greater than $r = 0.94$, and US-UMB showed both the strongest average correlation and smallest error among sites ($r = 0.97$, RMSE = 0.37). Mean seasonal trajectories of observed and predicted LAI were generally in good agreement with each other, as well as with LAI-2000 data (Fig. 4). The mean seasonal trajectories revealed that at Ca-Oas and US-Ha1 $L_{(T,P,D)}$ tended to underestimate LAI during the fall. By contrast, the remaining three sites showed a tendency to overestimate LAI in the spring.

3.2.3. Predicting phenological transition dates

Across all sites and years the mean (±1 SD) bias in the timing of spring thresholds was −10 (±14) days, with a consistent early bias occurring at each transition threshold [20% (−9 ± 16 days); 50% (−10 ± 13 days); 80% (−11 ± 14 days)]. The majority of sites showed an early mean bias for spring thresholds, with only Ca-Oas showing a neutral bias (0 ± 12 days). US-MMS had the largest average bias for spring transition thresholds, with each of the three transitions showing a large early bias [20% (−15 ± 9 days); 50% (−21 ± 9 days); 80% (−19 ± 7 days)]. The timing of fall thresholds were also early on average across all sites and years of data (−6 ± 15 days), with the 20% threshold having the largest bias (−14 ± 16 days). The most notable biases occurred at the fall 20% threshold at Ca-Oas (−19 ± 16 days) and US-Ha1. The latter was biased slightly less than four weeks early. The remaining three sites all performed favorably in predicting fall transition dates [US-MMS (+6 ± 10 days); US-UMB (+1 ± 7 days); US-WCr (0 ± 7 days)].

3.3. Site-specific estimation and best model formulation

In addition to finding the best study-wide model formulation and τ ($L_{(T,P,D)}$; $\tau = 0.39$), we also tested the model framework by parameterizing it at individual sites. This was done in two parts; first, τ was estimated for $L_{(T,P,D)}$ at each site, and second the combination of site-specific τ and best model formulation was chosen at each site based on AICc. The study-wide model performed well in terms of r and RMSE but as noted above it had a tendency towards: (1) overestimation of LAI and early bias in spring phenological transitions at US-MMS, US-UMB, and US-WCr, and (2) underestimation of LAI and early bias in phenological transitions at Ca-Oas and US-Ha1 in the fall. Consequently, the analysis of site-specific models was restricted to the areas where the study-wide model underperformed. Table 4 shows the site-specific values of τ and model selection for each of the sites.

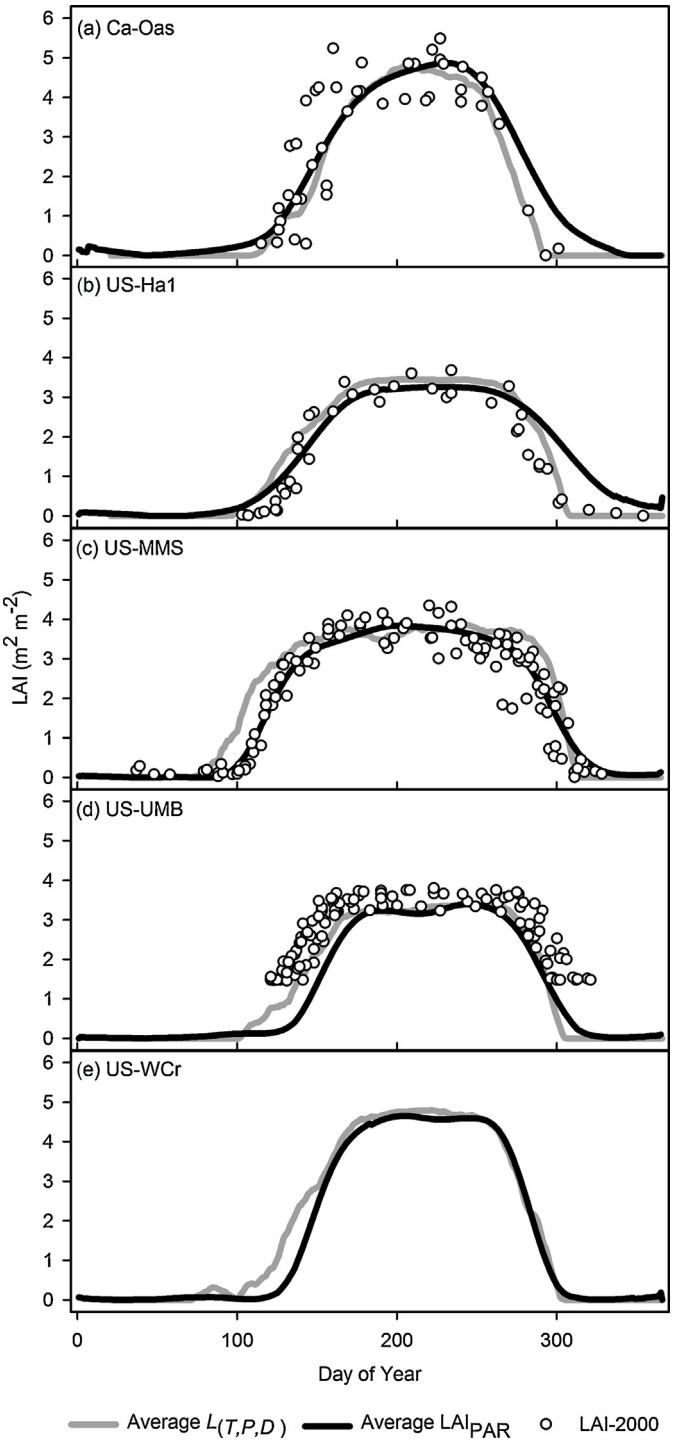

Fig. 4. Site long averages of both predicted and observed leaf area index (LAI). Continuous LAI observations were derived from the ratio of below canopy to above canopy PAR (LAI_{PAR}) and predicted LAI was modeled by rescaling the GSI phenology model to LAI. Open circles depict in situ LAI measurements taken with the LAI-2000 plant canopy analyzer. Values of predicted LAI are for the study-wide estimated parameter τ and model formulation ($L_{(T,P,D)}$; $\tau = 0.39$).

Table 4
Site-specific estimates of τ and the best site-specific formulation of the growing season index (GSI) for predicting leaf area index (LAI). For more information on model formulations refer to Table 2.

Site	Site-specific τ	Site-specific model formulation
Ca-Oas	0.19	$L_{(T)}$
US-Ha1	0.37	$L_{(T,D)}$
US-MMS	0.60	$L_{(T,P,D)}$
US-UMB	0.55	$L_{(T,D)}$
US-WCr	0.50	$L_{(T,P)}$

3.3.1. Site-specific estimation of τ

The mean difference between predicted LAI and LAI_{PAR} was calculated at daily time steps for each site in order to further examine the seasonal patterns of error in LAI estimation (Fig. 5). Unsurprisingly, this temporal view of error revealed that the greatest errors tended to occur in conjunction with the average timing of phenological transition dates derived from LAI_{PAR}. RMSE was calculated during spring and fall, defined as the periods between the 20% and 80% thresholds on the ascending and descending seasonal trajectory of LAI respectively. Site-specific τ estimation reduced RMSE during the spring at US-MMS, US-UMB, and US-WCr. Estimating τ at Ca-Oas reduced RMSE during the fall but failed to do so at US-Ha1. Both US-UMB and US-WCr had increased RMSE during the fall when using site-specific estimates of τ.

Mean study-wide values at individual transition thresholds showed no difference between the study-wide and site-specific τ values. At individual sites, however, the mean bias across spring phenological transition thresholds was reduced at US-MMS, US-UMB, and US-WCr (Table 5). All three sites had a reduction in bias of a week or more at the 20% spring threshold. Site-specific τ values reduced the mean bias across fall phenological transitions at Ca-Oas but had no influence at US-Ha1. The study-wide model had errors of 11 days or more for all sites when predicting the length of the growing season. Site-specific estimation of τ produced comparatively smaller bias in growing season length at all sites [Ca-Oas (-5 ± 27 days), US-Ha1 (-15 ± 15 days), US-MMS (-2 ± 15 days), US-UMB (-6 ± 9 days), US-WCr (5 ± 22 days)].

3.3.2. Site-specific model formulation

The selection of site specific model formulations did not further reduce springtime RMSE beyond the improvements already made by site-based τ estimation at any of the sites. Even though site-specific τ estimation did not substantially reduce fall RMSE at US-Ha1, the addition of site-specific model formulation reduced RMSE to 0.36. None of the sites benefited from site-specific model formulation for spring transition thresholds, but Ca-Oas and US-Ha1 both had reductions in mean bias of fall transitions. Across all sites and years the only transition thresholds that benefited from site-specific model selection were the fall 20% [site-specific model (-6 ± 17 days); site-specific τ (-15 ± 14 days)] and 50% [site-specific model (-3 ± 11 days); site-specific τ (-5 ± 11 days)] transition thresholds.

4. Discussion

4.1. Piecewise rescaling of LAI

The use of piecewise linear rescaling reduced RMSE between predicted LAI and observed LAI at all sites over linear rescaling. There was also substantial reduction in the mean bias across all phenological transition thresholds, especially the spring 20%, 50% and 80% thresholds. The timing of spring thresholds showed greater sensitivity in response to changes in τ than did fall. Since temperature is the most important factor driving seasonal canopy dynamics at these sites, this sensitivity may be explained by patterns in the temperature component of the GSI model framework ($f_1(T_a)$). We calculated a 21 day running mean of $f_1(T_a)$ for all sites and years of data and examined the average rate of change of the temperature index value during the spring and fall. The average slope of the temperature index was greater in the spring than in the fall for all sites. Because $f_1(T_a)$ is the largest component of the GSI framework driving canopy seasonality at our sites, and τ influences slope of the line used to rescale GSI to predicted LAI, it is reasonable to assume that the increased slope of the temperature index during the spring explains the greater sensitivity of spring to changes in τ.

4.2. Study-wide τ estimation and best model formulation

The study-wide model ($L_{(T,P,D)}$; $\tau = 0.39$) performed well on average at predicting in situ LAI-2000 measurements, and this is important because it demonstrated that it was able to mimic the same pattern and magnitude of observed LAI against an independent dataset. Although there was some disagreement between predicted LAI and LAI-2000 measurements at US-UMB (Fig. 3), the species composition of the site may provide some explanation as to the causes. The underpredicted values occurred during periods of deciduous dormancy at the start and end of the growing season and may be explained by the presence of white pine (*Pinus strobus*) in the understory at US-UMB, as noted in the data documentation, which resulted in higher measured LAI during these periods. The implementation of $L_{(T,P,D)}$ in this study was only intended to model deciduous canopy dynamics and thus reduces LAI to 0 during dormancy despite the presence of an evergreen understory.

The study-wide model showed strong correlations to LAI_{PAR} for all site years of data, but it would be misleading to only consider the strength of the overall correlation in assessing the model performance. While the model performed well when looking at the aggregated pool of data, it is not unexpected that performance would vary between sites when applying a generalized set of parameters. The mean seasonal trajectories of observed and predicted LAI revealed that several sites overestimated LAI during the spring or underestimated LAI in the fall. In addition, there was a tendency towards an early bias in all phenological transitions thresholds. Despite this overall trend towards early bias, the biases did not offset equally and lead to longer than observed predicted growing seasons at US-MMS ($+11 \pm 16$ days), US-UMB ($+13 \pm 17$ days), and US-WCr ($+22 \pm 23$ days). Ca-Oas (-22 ± 22 days) and US-Ha1 (-18 ± 15 days) both had substantially shorter growing seasons than observed.

4.3. Site-specific τ estimation and best model formulation

Overestimation of LAI at US-MMS, US-UMB, and US-WCr suggested that the study-wide τ was too low. Likewise, the underestimation of LAI at Ca-Oas and US-Ha indicated that the study-wide estimated τ was too high. The estimation of τ at each site confirmed that increasing τ reduced overprediction of LAI and decreasing τ reduced underprediction of LAI. Additionally, estimating τ on a site by site basis reduced the bias in phenological transition dates. Thus, by altering only a single parameter it was possible to address errors in both the magnitude of LAI and timing of phenological transition dates. Because all sites benefitted from estimation of τ, it would be useful to have an understanding of how the value of τ is related to conditions at a given site. Since τ influences the rate at which LAI increases in the spring, as well as the timing of leaf onset, it is reasonable to assume that there would be a relationship between the rate of green up and τ. We looked at the average number of days between the 20% and 80% spring transition thresholds derived from LAI_{PAR} in comparison to the estimated τ at each site. There was a general trend, with the exception of US-MMS, between decreased time between transition

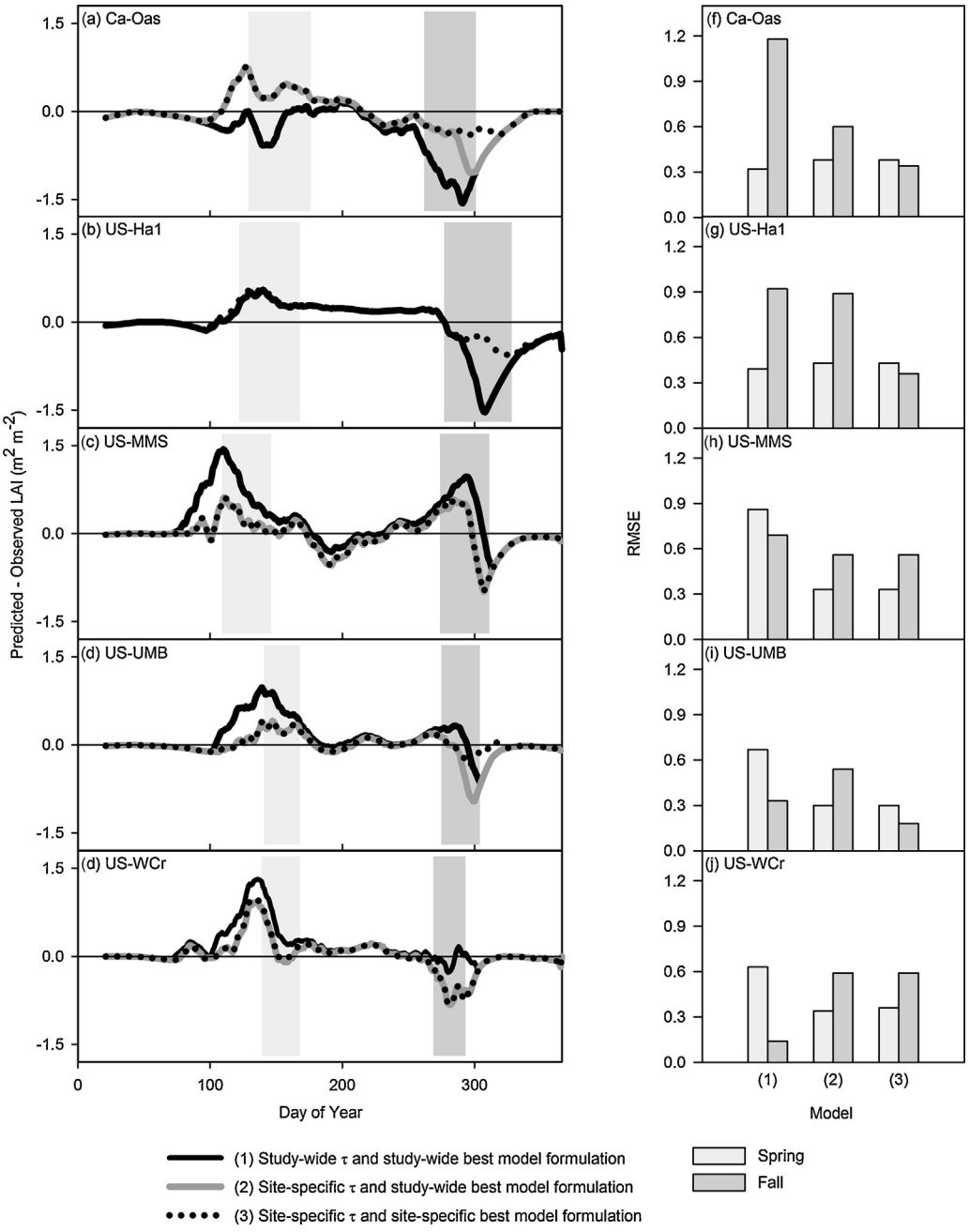

Fig. 5. Daily mean difference between predicted (L) and observed (LAI_{PAR}) leaf area index (LAI) (a–d). Negative values indicate that the model underestimated LAI. The study-wide model was estimated against the entire aggregated set of data ($L_{(T,P,D)}$; $\tau = 0.39$). LAI predictions using site-specific estimates of τ (solid gray line) and model formulation (dotted black line) are also presented. Spring (light gray plot area) and fall (medium gray plot area) were calculated from site long averages of the duration between the 20% and 50% phenological transition dates derived from LAI_{PAR}. Bar plots summarize the root mean squared error (RMSE) during the spring (light gray bar) and fall (medium gray bar) for each of the three models (f–j).

Table 5
Spring and fall bias in the date at which phenological transition thresholds were reached. Spring represents the mean bias across the 20%, 50%, and 80% phenological transition thresholds. Observed phenological transition dates were extracted from the time series of leaf area index (LAI) data derived from below canopy photosynthetically active radiation (PAR) sensors. A negative bias indicates that predicted transition dates were early. τ is the parameter used to rescale the growing season index (GSI) to LAI.

Site	Study-wide model		Site-specific τ		Site-specific model formulation	
	Spring	Fall	Spring	Fall	Spring	Fall
Ca-Oas	0 ± 12	−13 ± 15	−9 ± 13	−7 ± 14	−9 ± 13	−3 ± 16
US-Ha1	−9 ± 12	−12 ± 17	−10 ± 11	−12 ± 17	−10 ± 11	−4 ± 17
US-MMS	−18 ± 8	+6 ± 10	−7 ± 8	+1 ± 11	−7 ± 8	1 ± 11
US-UMB	−13 ± 11	+1 ± 7	−5 ± 6	−4 ± 7	−5 ± 6	0 ± 9
US-WCr	−17 ± 18	0 ± 7	−10 ± 15	−4 ± 7	−10 ± 15	−4 ± 7

thresholds and increased τ. Due to the small sample size in this study it is difficult to draw any broad conclusions about this relationship, but future research could expand to include a wider range of sites that encompass more variation in environmental conditions and seasonal canopy dynamics.

The addition of site-specific τ estimation helped to correct errors in both the predicted magnitude of LAI and the timing of phenological transition dates. Stöckli et al. (2008) used data assimilation to generate new parameters at individual sites for the components of the GSI framework in their PROGNOSTIC model. They compared PROGNOSTIC to in situ LAI measurements at US-MMS (r = 0.9, RMSE = 1.65) and our results were able to achieve nearly the same strength of correlation with less than half the error (r = 0.89, RMSE = 0.68). Additionally, they examined the bias in the timing of the 50% phenological transition threshold. PROGNOSTIC showed a bias of −12 days for the spring 50% threshold and +1 day in the fall at US-MMS. Our approach, using $L_{(T,P,D)}$ and site-specific τ, had a bias of −5 (± 9 days) in the spring and 2 (±5 days) in the fall at the same thresholds. $L_{(T,P,D)}$ was able to produce comparable results to PROGNOSTIC without a complex data assimilation model, and the estimation of only a single parameter.

The best model formulation selected across all sites was $L_{(T,P,D)}$ and this confirms that the framework proposed by Jolly et al. (2005) works best as a generalized model even across sites that are all primarily driven by temperature. When model formulation was assessed at individual sites, Ca-Oas was the only site that had a model comprised only of the temperature function. The selection of more complex models at the remaining sites demonstrates that the inclusion of additional environmental constraints improved upon a simple temperature only driven model. However, the selection of simpler model formulations at specific sites appears to be largely driven by model parsimony instead of performance. With the exception of US-Ha1, the combination of estimating both τ and model formulation at individual sites showed little improvement over τ estimation alone. These results suggest that it is possible to use more parsimonious models to predict LAI at individual sites without significant changes in accuracy when compared to the full formulation.

4.4. Methodological considerations

The mean seasonal trajectory of LAI_{PAR} revealed that at Ca-Oas, and US-Ha1 it tended to deviate from observed in situ LAI-2000 measurements. One possible explanation for this is that the upward facing PAR sensors at these sites are at a fixed location and LAI-2000 measurements are averaged over a spatially representative sample of the area. While it is mentioned in the data documentation for US-Ha1 that LAI-2000 measurements do indeed consist of a spatial average of measurements, we are uncertain if this is also the case at Ca-Oas. US-MMS was the only site that had multiple spatial locations of below canopy PAR sensors and it was also the site with the strongest correlation and lowest error when compared to LAI-2000 measurements (r = 0.96, RMSE = 0.41). This supports the idea that a more spatially representative sample of below canopy PAR data could help reduce errors between LAI_{PAR} and LAI-2000 measurements. A study conducted at US-Ha1 found that for red oak (*Quercus rubra*) there could be delays on the order of weeks to months from the time leaves turned brown to leaf abscission (Hadley et al., 2009). If the upward pointing PAR sensors observed trees that experience longer delays in abscission than is spatially representative at the site it could possible lead to a slower than expected rate of decline in the fall. One possible way to investigate these concerns would be to introduce an additional source of validation data in the form of near surface remote sensing platforms designed to capture canopy greenness.

4.5. Future research

Our study only tested the ability of the GSI framework to model LAI at deciduous broadleaf sites, none of which were moisture limited. In order to gain further insight into the widespread applicability of this framework additional research is needed on a larger representative sample of biomes, particularly ones which exhibit water stress. While the above and below canopy PAR data used as validation data in this study is only available at a select number of sites, other continuous measures of canopy dynamics could serve as validation data. The emergence of near-surface remote sensing is one promising option that can aid in validating phenological models (Richardson et al., 2009; Richardson et al., 2007; Sonnentag et al., 2012). Using near-surface remote sensing would also allow for testing in other environments, such as grasslands, where deriving LAI from PAR differencing is not suitable. The use of vegetation indices from near surface remote sensing may also be more applicable to assess evergreen forests, since changes in canopy LAI are less pronounced than deciduous sites. By expanding the type of validation datasets used it should be possible to include a larger number of sites, and also a wider range of environmental conditions. A more representative sample of site conditions could allow for the examination between τ and the length of green up. If a mechanistic, rather than empirical link, could be found then our model framework could retain flexibility and accuracy for making predictions under future conditions. Ideally an integrative approach with field data, near-surface remote sensing, flux data, and remote sensing data could be used to validate model performance locally at selected sites and then expand outwards to a global analysis at sites without a full complement of data sources.

4.6. Implications

Poor representation of seasonal canopy dynamics within models can lead to errors in modeled productivity (Kucharik et al., 2006; Ryu et al., 2008). In an analysis of 14 terrestrial biosphere models Richardson et al. (2012) found that modeled errors in the seasonal dynamics of gross ecosystem productivity (GEP) were largely a result of poorly modeled seasonal dynamics of LAI. We show that using a piecewise linear function for rescaling GSI to LAI can reduce errors in modeled LAI over a simple linear rescaling. Additionally, errors in the seasonality of LAI were further reduced by performing parameter estimation of τ at individual sites. Gu et al. (2003) note that annual carbon assimilation is influenced by the speed at which plants reach peak rates of assimilation. In our study of temperature driven sites τ was able to change both the timing of phenological transitions and the rate of change in LAI. The rate of green up showed greater sensitivity to changes in τ compared to the rate of senescence, primarily due to seasonal patterns of the temperature component of GSI at our sites. Since τ can be used to modify the predicted rate of LAI accumulation in the spring, our approach shows the potential to mitigate errors in modeled productivity that result from poor representation of spring accumulation of LAI.

5. Conclusions

In this study we tested the ability of a prognostic phenology model to predict the seasonal course of LAI. To do this we developed a simple piecewise linear function, with a single parameter denoted as τ, to leverage the GSI model into a prognostic model of LAI. We also performed parameter estimation and sensitivity analysis of the influence of τ on predicting the seasonal course of LAI and the timing of phenological transition dates.

The value of τ influenced not only the timing of leaf expansion and senescence, but also the rate at which the canopy accumulated

LAI during green up and reduced LAI during senescence. Our results show that using τ to perform a piecewise linear rescaling of GSI to LAI reduced error from a strictly linear rescaling scheme. We found that spring was more sensitive to changes in τ than fall, largely attributed to the comparatively steeper slope of the temperature function of GSI during spring. Estimation of site-specific τ showed improvement over a single study-wide value estimated across all sites and helped to remedy errors in both the seasonality of LAI and the timing of phenological transitions.

In addition to parameter estimation, we also tested a number of model formulations of the GSI framework to test for improvement over a solely temperature driven model. Study-wide analysis revealed that the full formulation of the GSI framework performed best, which is unsurprising given conception as a generalized model. At individual sites only a single site selected the full formulation of GSI as a best model. The selection of other models was largely a result of model parsimony, instead of model improvement. This suggests that many sites may be able to use more parsimonious models to estimate prognostic LAI without significant differences in accuracy from the full GSI formulation.

Accurate representation of canopy seasonality is needed to reduce errors and uncertainties in modeled predictions of vegetation productivity. We show that it is possible to reduce errors in predicted LAI and the timing of phenological transition dates with the estimation of a single parameter. Our approach produced mean seasonal trajectories of LAI that closely match those at 5 temperature driven deciduous broadleaf sites. Additional work is needed to examine the applicability to other sites, particularly ones that are not temperature drive, and to determine if there is any relationship between τ and the vegetation or environmental characteristics of sites.

Acknowledgements

We thank the AmeriFlux and Fluxnet-Canada PIs who provided the data on which our analysis was based. We would also like to thank the anonymous reviewers for their comments that greatly improved the content of the manuscript. Finally, we would like to give special thanks to Mike Habberfield and Jonathan Pleban for their feedback on a draft manuscript, and Matt Jolly for his assistance and correspondence regarding his model.

References

Barr, A.G., et al., 2004. Inter-annual variability in the leaf area index of a boreal aspen-hazelnut forest in relation to net ecosystem production. Agric. For. Meteorol. 126 (3–4), 237–255.
Barr, A.G., et al., 2007. Climatic controls on the carbon and water balances of a boreal aspen forest, 1994-2003. Global Change Biol. 13 (3), 561–576.
Black, T.A., et al., 2000. Increased carbon sequestration by a boreal deciduous forest in years with a warm spring. Geophys. Res. Lett. 27 (9), 1271–1274.
Blanken, P.D., Black, T.A., 2004. The canopy conductance of a boreal aspen forest, Prince Albert National Park, Canada. Hydrol. Process. 18 (9), 1561–1578.
Burnham, K.P., 2002. Model Selection and Multimodel Inference: A Practical Information–Theoretic Approach. Springer, New York, NY.
Campbell, G.S., Norman, J.M., 1998. An Introduction to Environmental Biophysics, xxi. Springer, New York, NY, pp. 286.
Chen, J.M., Black, T.A., 1992. Defining leaf-area index for non-flat leaves. Plant Cell Environ. 15 (4), 421–429.
Chen, J.M., et al., 2002. Derivation and validation of Canada-wide coarse-resolution leaf area index maps using high-resolution satellite imagery and ground measurements. Remote Sens. Environ. 80 (1), 165–184.
Cook, B.D., et al., 2004. Carbon exchange and venting anomalies in an upland deciduous forest in northern Wisconsin USA. Agric. For. Meteorol. 126 (3–4), 271–295.
De Kauwe, M.G., Disney, M.I., Quaife, T., Lewis, P., Williams, M., 2011. An assessment of the MODIS collection 5 leaf area index product for a region of mixed coniferous forest. Remote Sens. Environ. 115 (2), 767–780.
Dragoni, D., et al., 2011. Evidence of increased net ecosystem productivity associated with a longer vegetated season in a deciduous forest in south-central Indiana, USA. Global Change Biol. 17 (2), 886–897.
Fang, H.L., Wei, S.S., Liang, S.L., 2012. Validation of MODIS and CYCLOPES LAI products using global field measurement data. Remote Sens. Environ. 119, 43–54.
Fitzjarrald, D.R., Acevedo, O.C., Moore, K.E., 2001. Climatic consequences of leaf presence in the eastern United States. J. Clim. 14 (4), 598–614.
Gough, C.M., et al., 2013. Sustained carbon uptake and storage following moderate disturbance in a Great Lakes forest. Ecol. Appl. 23 (5), 1202–1215.
Groenendijk, M., et al., 2011. Seasonal variation of photosynthetic model parameters and leaf area index from global Fluxnet eddy covariance data. J. Geophys. Res. Biogeosci. 116 (G4), G04027.
Gu, L., et al., 2003. Phenology of vegetation photosynthesis. In: Schwartz, M. (Ed.), Phenology: An Integrative Environmental Science. Tasks for Vegetation Science. Springer, Netherlands, pp. 467–485.
Hadley, J.L., O'Keefe, J., Munger, J.W., Hollinger, D.Y., Richardson, A.D., 2009. Phenology of forest–atmosphere carbon exchange for deciduous and coniferous forests in southern and northern New England: variation with latitude and landscape position. In: Phenology of Ecosystem Processes: Applications in Global Change Research. Springer, New York, pp. 119–141.
Hunter, A.F., Lechowicz, M.J., 1992. Predicting the timing of budburst in temperate trees. J. Appl. Ecol. 29 (3), 597–604.
Jeong, S.J., Medvigy, D., Shevliakova, E., Malyshev, S., 2012. Uncertainties in terrestrial carbon budgets related to spring phenology. J. Geophys. Res. Biogeosci. 117 (G1), G01030.
Jolly, W.M., Nemani, R., Running, S.W., 2005. A generalized, bioclimatic index to predict foliar phenology in response to climate. Global Change Biol. 11 (4), 619–632.
Kucharik, C.J., et al., 2006. A multiyear evaluation of a dynamic global vegetation model at three AmeriFlux forest sites: vegetation structure, phenology, soil temperature, and CO_2 and H_2O vapor exchange. Ecol. Modell. 196 (1–2), 1–31.
Levis, S., Bonan, G.B., 2004. Simulating springtime temperature patterns in the community atmosphere model coupled to the community land model using prognostic leaf area. J. Clim. 17 (23), 4531–4540.
Lieth, H., 1974. Phenology and Seasonality Modeling. Springer, New York, NY, pp. 444.
Melaas, E.K., et al., 2013. Using FLUXNET data to improve models of springtime vegetation activity onset in forest ecosystems. Agric. For. Meteorol. 171, 46–56.
Menzel, A., et al., 2006. European phenological response to climate change matches the warming pattern. Global Change Biol. 12 (10), 1969–1976.
Moore, K.E., et al., 1996. Seasonal variation in radiative and turbulent exchange at a deciduous forest in central Massachusetts. J. Appl. Meteorol. 35 (1), 122–134.
Moulin, S., Kergoat, L., Viovy, N., Dedieu, G., 1997. Global-scale assessment of vegetation phenology using NOAA/AVHRR satellite measurements. J. Clim. 10 (6), 1154–1170.
Myneni, R.B., Keeling, C.D., Tucker, C.J., Asrar, G., Nemani, R.R., 1997. Increased plant growth in the northern high latitudes from 1981 to 1991. Nature 386 (6626), 698–702.
Parmesan, C., 2006. Ecological and evolutionary responses to recent climate change. In: Annual Review of Ecology Evolution and Systematics. Annual Reviews, Palo Alto, CA, pp. 637–669.
Randerson, J.T., Thompson, M.V., Conway, T.J., Fung, I.Y., Field, C.B., 1997. The contribution of terrestrial sources and sinks to trends in the seasonal cycle of atmospheric carbon dioxide. Global Biogeochem. Cycles 11 (4), 535–560.
Reed, B.C., et al., 1994. Measuring phenological variability from satellite imagery. J. Veg. Sci. 5 (5), 703–714.
Richardson, A.D., et al., 2012. Terrestrial biosphere models need better representation of vegetation phenology: results from the North American Carbon Program Site Synthesis. Global Change Biol. 18 (2), 566–584.
Richardson, A.D., et al., 2010. Influence of spring and autumn phenological transitions on forest ecosystem productivity. Philos. Trans. R. Soc., Ser. B 365 (1555), 3227–3246.
Richardson, A.D., Braswell, B.H., Hollinger, D.Y., Jenkins, J.P., Ollinger, S.V., 2009. Near-surface remote sensing of spatial and temporal variation in canopy phenology. Ecol. Appl. 19 (6), 1417–1428.
Richardson, A.D., et al., 2007. Use of digital webcam images to track spring green-up in a deciduous broadleaf forest. Oecologia 152 (2), 323–334.
Ryu, S.R., Chen, J., Noormets, A., Bresee, M.K., Ollinger, S.V., 2008. Comparisons between PnET-Day and eddy covariance based gross ecosystem production in two Northern Wisconsin forests. Agric. For. Meteorol. 148 (2), 247–256.
Sakai, R.K., Fitzjarrald, D.R., Moore, K.E., 1997. Detecting leaf area and surface resistance during transition seasons. Agric. For. Meteorol. 84 (3–4), 273–284.
Schmid, H.P., Grimmond, C.S.B., Cropley, F., Offerle, B., Su, H.B., 2000. Measurements of CO_2 and energy fluxes over a mixed hardwood forest in the mid-western United States. Agric. For. Meteorol. 103 (4), 357–374.
Schwartz, M.D., Ahas, R., Aasa, A., 2006. Onset of spring starting earlier across the Northern Hemisphere. Global Change Biol. 12 (2), 343–351.
Sonnentag, O., et al., 2012. Digital repeat photography for phenological research in forest ecosystems. Agric. For. Meteorol. 152, 159–177.
Stöckli, R., et al., 2008. Remote sensing data assimilation for a prognostic phenology model. J. Geophys. Res. Biogeosci. 113 (G4), G04021.
Thompson, S.E., et al., 2011. Comparative hydrology across AmeriFlux sites: the variable roles of climate, vegetation, and groundwater. Water Resour. Res. 47 (10), W00J07.
Urbanski, S., et al., 2007. Factors controlling CO_2 exchange on timescales from hourly to decadal at Harvard Forest. J. Geophys. Res. Biogeosci. 112 (G2), G02020.

White, M.A., et al., 2009. Intercomparison, interpretation, and assessment of spring phenology in North America estimated from remote sensing for 1982–2006. Global Change Biol. 15 (10), 2335–2359.
White, M.A., Thornton, P.E., Running, S.W., 1997. A continental phenology model for monitoring vegetation responses to interannual climatic variability. Global Biogeochem. Cycles 11 (2), 217–234.
Wythers, K.R., Reich, P.B., Turner, D.P., 2003. Predicting leaf area index from scaling principles: corroboration and consequences. Tree Physiol. 23 (17), 1171–1179.
Zhang, Y.Z., Qu, Y.H., Wang, J.D., Liang, S.L., Liu, Y., 2012. Estimating leaf area index from MODIS and surface meteorological data using a dynamic Bayesian network. Remote Sens. Environ. 127, 30–43.